Observation and simulation of the energy levels of the trivalent thulium ion in gadolinium oxychloride

1995 J. Phys.: Condens. Matter 7 5127

(http://iopscience.iop.org/0953-8984/7/26/018)

J. Phys.: Condens. Matter 7 (1995) 5127–5138. Printed in the UK

Observation and simulation of the energy levels of the trivalent thulium ion in gadolinium oxychloride

Jorma Hölsä†, Ralf-Johan Lamminmäki†, Elisabeth Antic-Fidancev‡, Michèle Lemaitre-Blaise‡ and Pierre Porcher‡

† University of Turku, Department of Chemistry, FIN-20500 Turku, Finland
‡ CNRS, UPR 209, 1, Place A Briand, F-92195 Meudon, France

Received 4 January 1995, in final form 13 March 1995

Abstract. The optical absorption of the Tm^{3+} ion in the gadolinium oxychloride (GdOCl) matrix in the UV, visible, and NIR range was studied at temperatures between 9 and 300 K. The visible luminescence of GdOCl:Tm^{3+} under Ar^+ ion laser and mercury lamp excitation was recorded at 9, 77, and 300 K, too. The crystal field (CF) splitting of the $^3H_{4-6}$, $^3F_{2-4}$, $^1G_4$, $^1D_2$, and $^1I_6$ levels of the Tm^{3+} ion deduced from the spectra was analysed according to the C_{4v} point symmetry of the RE^{3+} site. The resulting energy level scheme, consisting of 39 levels (i.e. 55 Stark components) out of the total of 70 (91) for the whole $4f^{12}$ configuration, was simulated with the aid of a phenomenological theory taking simultaneously into account both the free-ion and CF effects. The model included 13 adjustable parameters describing the electrostatic (the Racah parameters E_{0-3}) and the configuration interaction (the Trees parameters α, β, and γ) as well as the spin–orbit coupling (the coupling constant ζ_{4f}). The CF effect was accounted for by the five non-zero B_q^k parameters B_0^2, B_0^4, B_4^4, B_0^6, and B_4^6. Good simulation of the experimental energy level scheme was achieved with a root mean square deviation equal to 21 cm^{-1}. A comparison to the energy level parametrization of the Pr^{3+} ($4f^2$), Nd^{3+} ($4f^3$), Eu^{3+} ($4f^6$), and Tb^{3+} ions ($4f^8$ electron configuration) in other REOCl matrices shows the consistency of the present results. The systematic trends in the CF effect on the energy level schemes of the RE^{3+} ions are discussed, too.

1. Introduction

The study of the spectroscopic properties of the Tm^{3+} ion in solid state materials has attracted rather modest attention probably due to the lack of potential applications. The use of LaOBr:Tm^{3+} as the effective phosphor in x-ray image-intensifying screens may be the only current utilization based on the spectroscopic properties of this RE^{3+} ion [1]. Some other applications such as the Cr^{3+}- and Tm^{3+}-codoped $Y_3Al_5O_{12}$ (YAG) as a laser material [2] and the Yb^{3+}- and Tm^{3+}-codoped materials as IR to visible converters [3] have been proposed.

For many applications, e.g. for the study of the sensitizer to activator energy transfer, it is important to know the detailed energy level scheme of the RE^{3+} in the appropriate host matrix. Well established investigations of the energy level scheme of the Tm^{3+} ion in various host matrices are, however, rather scarce. Detailed characterization of the interactions effective in the formation of the energy level scheme of the Tm^{3+} ion has been carried out mostly for the simple fluorides LaF_3 [4, 5], $LiYF_4$ [6, 7], and CaF_2 [8], chlorides $LaCl_3$ [9, 10], YCl_3 [11], and $TmCl_3 \cdot 6H_2O$ [12, 13], oxide Y_2O_3 [14], as well as for the mixed oxide $YAlO_3$ [15, 16] and $Y_3Al_5O_{12}$ (YAG) [17] hosts. The Tm^{3+} energy level scheme has also been studied for other oxidic matrices YVO_4 [18], YPO_4 [19], $CaWO_4$ [20], and

$Tm(C_2H_5SO_4)_3 \cdot 9H_2O$ [21] as well as for ZnS [22]. The emission and excitation spectra as well as an incomplete crystal field (CF) analysis of the Tm^{3+} ion in the LaOBr matrix have been presented earlier [23]. Only in a few cases has the number of CF levels involved in the study approached the maximum degeneracy of the $4f^{12}$ electron configuration of the Tm^{3+} ion. Nevertheless, the total degeneracy of 91, which is rather low for an RE^{3+} ion, can be treated theoretically and by computational means easily as a whole without any truncations.

In this paper the optical UV, visible, and NIR absorption spectra of the Tm^{3+} ion in the GdOCl matrix are presented in the temperature range between 9 and 300 K. Together with the visible luminescence spectra of the Tm^{3+}-doped GdOCl at 9, 77, and 300 K, the optical data are interpreted in terms of the C_{4v} point symmetry of the RE^{3+} site in the tetragonal REOCl matrix using the multipolar and group theoretical selection rules for electronic transitions. The energy levels are labelled with the appropriate irreducible representations of the C_{4v} point group. The experimental values for the energy levels are compared with the calculated ones obtained by a phenomenological model comprising a Hamiltonian which includes the electrostatic, spin–orbit, interconfigurational, and CF interactions. The simultaneous treatment of the free-ion and CF interactions within the $4f^{12}$ electron configuration yielded a satisfactory agreement with the experimental values of 55 Stark components as the low RMS deviation of 21 cm^{-1} indicates. The CF parameter set obtained was found to be consistent with the results of the previous studies on the corresponding REOCl (or REOCl:RE^{3+}) systems [24–27]. The slight differences were correlated to the trends anticipated for the evolution of the CF effect across the RE^{3+} series.

2. Experimental details

2.1. Sample preparation

The GdOCl:Tm^{3+} powder samples were prepared by the solid state reaction between NH_4Cl (with an excess of 7.5 per cent) and the homogeneous RE_2O_3 mixture in static N_2 atmosphere. Though the reaction between RE_2O_3 and NH_4Cl takes place at low temperature, $\sim$ 470 K [28], the powder samples were annealed at 1220 K in order to improve their crystallinity. For optical absorption measurements, the pure GdOCl samples were doped with the Tm^{3+} ion up to a rather high concentration, 9 mol% (based on the total RE^{3+} amount). The concentration of the dopant was 1 mol% in the GdOCl matrix aimed at luminescence studies in order to avoid the concentration quenching of luminescence.

The purity of the products was verified by routine XRD powder analysis. Although the heavier RE oxychlorides beyond ErOCl possess a different crystal structure from that of the lighter ones [29], no separation of two oxychloride phases was observed for GdOCl:Tm^{3+} in good agreement with Vegard's rule [30]. However, the lines in the optical absorption spectra were found to be rather large, possibly indicating some kind of local distortion. In fact, it was found that the solid solubility of the Tm^{3+} ion in the GdOCl host matrix is very limited indeed, since a phase separation occurred already above the Tm^{3+} concentration of 12 mol%.

2.2. *Optical measurements*

The optical absorption spectra of the Tm^{3+}-doped GdOCl were obtained with Cary 2400 and Cary 5E apparatuses in the near-IR, visible, and UV range. All absorption measurements were carried out at selected temperatures between 9 and 300 K in the wavelength range from 200 to 2300 nm (50 000 to 4350 cm^{-1}). The instruments were equipped with autocalibration

of the wavelength scale which resulted in the reproducibility of the measurements being better than 2 Å. The band width of 0.6 Å used in measurements was sufficient taking into account the width of the absorption lines.

The luminescence spectra of the GdOCl:Tm^{3+} powder samples were measured at 9, 77, and 300 K under Spectra Physics 164 Ar^+ ion laser or mercury lamp excitation and detected through a 1 m Jarrell–Ash monochromator with a Hamamatsu R374 photomultiplier connected to standard electronic treatment of the data. The maximum resolution of the set-up was around 1 cm^{-1}. The immersion-type Dewar cryostat ensured the sample temperature was kept constant at the boiling point of liquid nitrogen. The helium cryostats allowed the sample temperature to be varied continuously between 9 and 300 K for both the absorption and luminescence measurements.

2.3. Structural data

The crystal structure of REOCl (RE = La–Er, and Y) belongs to the tetragonal system with $P4/nmm$–D_{4h}^7 (No 129 [31]) as the space group [32]. The unit cell of the Matlockite-type PbFCl structure contains two formula units. The overall crystal structure consists of alternating layers of the $[REO]_n^{n+}$ complex cations and the Cl^- anions typical of the tetragonal RE oxycompounds [33]. The RE^{3+} cation is coordinated to four oxygens and five chlorines in a monocapped square antiprism arrangement. This coordination yields C_{4v} as the point symmetry of the RE^{3+} site as shown in the inset of figure 2. In contrast to the lighter members of the REOCl series, the oxychlorides beyond ErOCl crystallize in the hexagonal system with $R\bar{3}m$–D_{3d}^5 (No 166 [31] $Z = 6$) as the space group [34]. The point symmetry of the RE^{3+} site in this SmSI-type structure is C_{3v} originating from an approximate tricapped prismatic coordination to five chlorines and four oxygens. The YOCl and ErOCl have been reported to be dimorphic possessing both crystal structures [35].

One of the aims of the present investigation was to study the systematic trends in the free-ion and CF effects on the energy level schemes in the whole RE^{3+} series in the tetragonal REOCl structure. The hexagonal crystal structure of TmOCl prevented the use of the pure compound to measure the absorption spectra. Accordingly, GdOCl samples doped with 1 to 9 mol% of Tm^{3+} were used instead of the pure TmOCl. The concentration range had to be chosen carefully to obtain concentrations low enough to respect Vegard's rule.

3. Results and discussion

3.1. Theoretical background

The principal interactions in the free-ion electron structure of the RE^{3+} ions within the $4f^N$ configuration include the electrostatic repulsion between the 4f electrons (except for $4f^1$ and $4f^{13}$) and the coupling of their spin and orbital angular momentum. The two-body interactions may be taken into account for the configurations from $4f^2$ to $4f^{12}$ but they contribute only slightly to the total Hamiltonian [36]. In addition to the free-ion interactions, the CF effect must be incorporated when dealing with the solid state. The correct procedure for the simulation of the energy level schemes of the RE^{3+} ions involves the simultaneous treatment of both the free-ion and CF effects using the untruncated basis set of wave functions [37]. The effect of the free-ion interactions on the energy level scheme of the $4f^N$ configuration can be described by the Hamiltonian [36]

$$H_{FI} = H_0 + \sum_{k=0,1,2,3} E_k(nf, nf)e^k + \zeta_{4f}A_{SO} + \alpha L(L+1) + \beta G(G_2) + \gamma G(R_7). \qquad (1)$$

Expression (1) includes the spherically symmetric, one-electron term H_0, the electrostatic interaction between the equivalent 4f electrons (the Racah parameters E_k), the spin–orbit interaction (the coupling constant ζ_{4f}), and the terms accounting for the two-body correction terms (Trees parameters α, β, and γ [36]). The e^k, A_{SO}, L, $G(G_2)$, and $G(R_7)$ denote the corresponding effective operators.

The one-electron CF Hamiltonian H_{CF} incorporates the effect of the Coulombic interactions which arise from the surrounding charges on the 4f electrons of the RE^{3+} ion and can be written as follows [36]:

$$H_{CF} = \sum_{k=2}^{4,6} \sum_{q=0}^{k} \sum_{i=1}^{N} [B_q^k (C_q^k(i) + (-1)^q C_{-q}^k(i)) + iS_q^k (C_q^k(i) - (-1)^q C_{-q}^k(i))] \qquad (2)$$

where C_q^k are related to the spherical tensors of rank k, dependent on the coordinates of the ith electron with summation over all 4f electrons. B_q^k and S_q^k are the non-zero real and imaginary parts of the CF parameters, respectively. The number of the B_q^k (and S_q^k) parameters is defined by the site symmetry of the RE^{3+} ion [38]. In the case of the rather high C_{4v} site symmetry in REOCl, the number of the CF parameters is restricted to only five real ones, i.e. B_0^2, B_0^4, B_4^4, B_0^6, and B_4^6.

For low symmetries, i.e. C_1 and C_i, the simulation of the energy level scheme of the $4f^{12}$ configuration requires a diagonalization of a 91×91 square matrix which, however, can be treated on an ordinary PC without difficulties. The whole matrix can be divided for high point symmetries into several submatrices, e.g. into three matrices of dimensions of 25, 21 (a double matrix), and 24 for the C_{4v} symmetry, hence facilitating and accelerating the calculations. The B_q^k parameters were obtained by a least-squares fitting procedure between the experimental and calculated energy level values by minimizing the mean square deviation σ [39].

3.2. Interpretation of spectroscopic data

The Tm^{3+} ion possesses the $[Xe]4f^{12}$ ground configuration with total degeneracy of only 91. Moreover, this configuration extends in the solid state only to about 40 000 cm^{-1} with the exception of the $^1S_0$ level at $\sim$ 74 000 cm^{-1} [11]. Hence all CF levels (except $^1S_0$) may be determined either from the traditional absorption and/or luminescence measurements. The lowest level of the charge transfer states (CTS)—corresponding to a transfer of an electron from either the oxygen or chlorine ligand to the Tm^{3+} ion—is situated in the GdOCl matrix above 35 000 cm^{-1}. The $4f^{12}$ ground configuration gives rise to 13 $^{2S+1}L_J$ levels ($^3H_{4-6}$, $^3F_{2-4}$, $^3P_{0-2}$, $^1D_2$, $^1G_4$, $^1I_6$, and $^1S_0$) only nine of which are situated below this threshold and are accessible by the one-photon absorption or luminescence spectroscopy. The transitions within the $4f^{12}$ configuration which overlap with the strong CTS bands are too weak as forbidden intraconfigurational transitions to be observed directly in the GdOCl matrix.

The CF effect lifts the $(2J + 1)$ degeneracy of the $^{2S+1}L_J$ free-ion levels to an extent determined by the crystal structure of the host lattice. For the C_{4v} site symmetry appropriate to the GdOCl matrix, the 13 $^{2S+1}L_J$ levels of the Tm^{3+} ion are split into 70 CF levels characterized by the irreducible representations A_1, A_2, B_1, B_2, and E (table 1) [38]. The $^{2S+1}L_J \rightarrow {}^{2S'+1}L'_{J'}$ transitions have multipolar character, i.e. they are induced by electric and/or magnetic dipole interactions. In general, the magnetic dipole transitions have close to negligible intensity when compared to those induced by the electric dipole interaction. Notable exceptions to this rule are found in the luminescence spectra of the Eu^{3+} ion where,

Table 1. The composition of the $^{2S+1}L_J$ levels of the Tm^{3+} ion ($4f^{12}$ electron configuration) for the C_{4v} point symmetry group.

$^{2S+1}L_J$ level	A_1	A_2	B_1	B_2	E
$J = 0$	1				
1		1			1
2	1		1	1	1
3		1	1	1	2
4	2	1	1	1	2
5	1	2	1	1	3
6	2	1	2	2	3
Total for Tm^{3+} ($4f^{12}$)	16	9	12	12	21

e.g. the $^5D_0 \rightarrow {}^7F_1$ transition usually has intensity comparable to that of the electric dipole transitions [26, 40, 41].

The free-ion selection rules for the electric and magnetic dipole transitions yield $\Delta J \leqslant 6$ and $\Delta J = 0, \pm 1$ for the allowed change in the quantum number J, respectively. The J mixing by the CF effect lifts partially the restrictions imposed by the free-ion selection rules. The following group theoretical selection rules for the pure electronic transitions between the Stark components are left as the only valid ones: (i) for the electric dipole transitions: $A_1 \rightarrow A_1$, $A_2 \rightarrow A_2$, $B_1 \rightarrow B_1$, $B_2 \rightarrow B_2$, and A_1, A_2, B_1, B_2, or $E \leftrightarrow E$, and (ii) magnetic dipole transitions: $A_1 \leftrightarrow A_2$, $B_1 \leftrightarrow B_2$, and A_1, A_2, B_1, B_2, or $E \leftrightarrow E$ [38]. Due to the powder samples, no polarization of the emission or absorption lines can be detected which leaves in occasional cases some ambiguity in the level assignments. For instance, the B_1 and B_2 levels could not be distinguished and are hence denoted further on by B' and B'' where B' (B'') can be either B_1 or B_2 (B_2 or B_1).

3.2.1. Luminescence spectra. The Ar^+ ion laser line at 457.9 nm excites effectively the $^1G_4$ level of the Tm^{3+} ion. At low temperatures the excitation relaxes mainly radiatively as luminescence. The non-radiative pathway through the multiphonon de-excitation to the $^3F_2$ level is inefficient owing to the large energy gap, $\sim 6000\ cm^{-1}$, between the two levels. The energy gap counts up to more than ten times the highest-energy lattice phonon available in the GdOCl matrix [42]. Other non-radiative processes such as the cross-relaxation of the excitation are expected to be improbable owing to the low concentration (1 mol%) of the Tm^{3+} ion. At higher concentrations, the $^1G_4 \rightarrow {}^3F_2$ to $^3H_6 \rightarrow {}^3F_4$ cross-relaxation might play a non-negligible role in the quenching of the emission from the $^1G_4$ level in some specific lattices where an energy match occurs between these four levels.

The easy interpretation of the electronic transitions between the different free-ion $^{2S+1}L_J$ levels in both the absorption and luminescence spectra is also facilitated by the close to complete absence of vibronic structure. This is in drastic contrast with the abundant vibronic fine structure found in the spectra of REOCl:Pr^{3+} [24]. The present observation is in agreement with the decrease in the probability of vibronic transitions with increasing atomic number of the RE^{3+} ion found elsewhere [43].

The visible luminescence of GdOCl:Tm^{3+} with laser excitation comprises hence the $^1G_4 \rightarrow {}^3F_4$ and $^1G_4 \rightarrow {}^3H_6$ transitions whereas only the $^1D_2 \rightarrow {}^3F_4$ transition was observed with UV excitation. The evolution of the $^1G_4 \rightarrow {}^3F_4$ transitions as a function of the temperature is reproduced in figure 1. This transition is the most intense one and is hence exploited in commercial applications as a blue emitting phosphor matching the blue sensitive films used in the x-ray intensifying screens [1]. The analysis of the spectra gave only partially the CF fine structure of the $^1D_2$, $^1G_4$, $^3F_4$, and $^3H_6$ levels. The assignment of

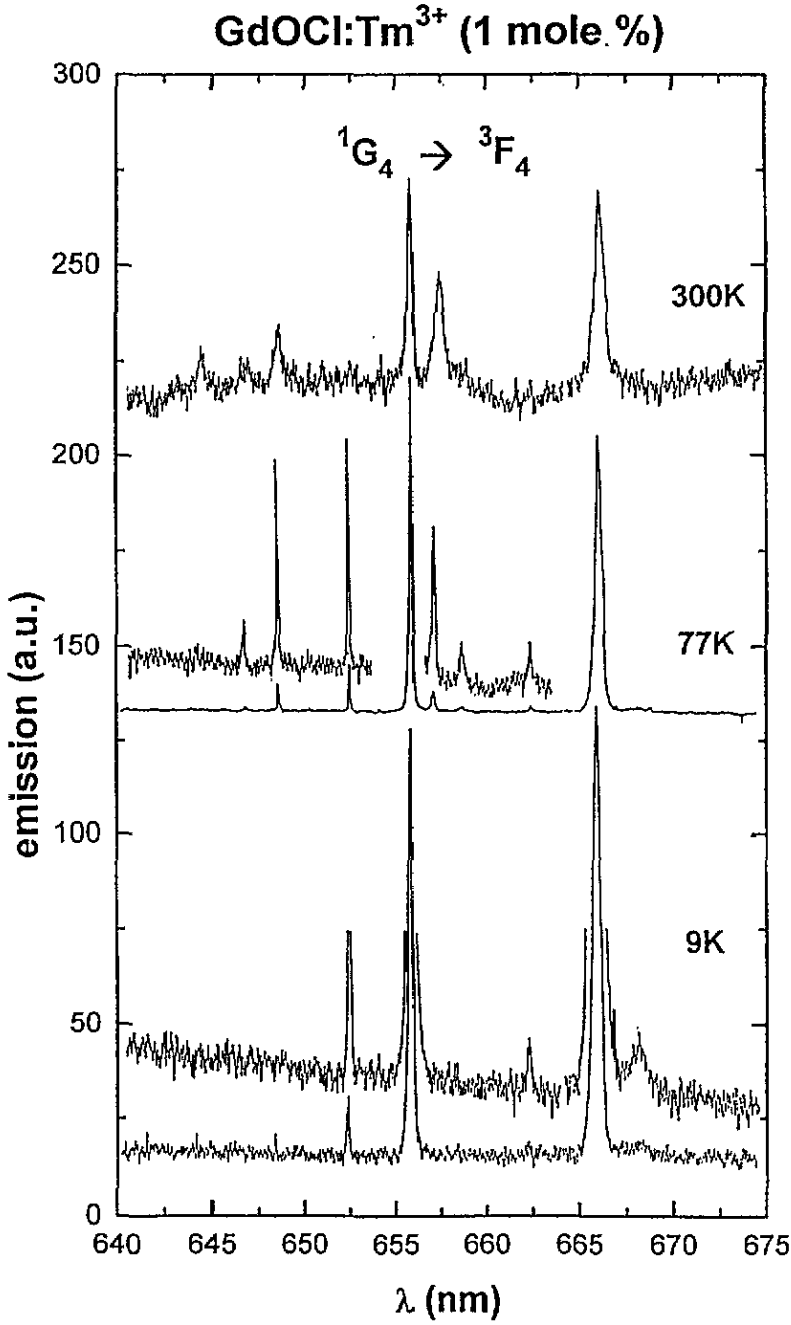

Figure 1. Part of the luminescence spectrum of $GdOCl:Tm^{3+}$ ($x_{Tm} = 0.01$) at 9, 77, and 300 K under Ar^+ ion laser excitation ($\lambda_{ex} = 457.9$ nm).

the energy levels to their appropriate irreducible representations was carried out by the group theoretical selection rules observed in the spectra and by the utilization of preliminary CF calculations based on the previous analyses of the $GdOCl:Eu^{3+}$ and $GdOCl:Tb^{3+}$ systems [26, 27].

3.2.2. Absorption spectra. The absorption spectrum of GdOCl:Tm^{3+} between 200 and 2300 nm (50 000 and 4350 cm^{-1}) was measured at selected temperatures between 9 and 300 K. At this region the absorption takes place from the ground $^3H_6$ level to the excited $^3F_4$, $^3H_5$, $^3H_4$, $^3F_3$, $^3F_2$, $^1G_4$, $^1D_2$, and $^1I_6$ levels as shown by a part of the absorption spectrum recorded at 9 K (figure 2). Although all transitions from the ground $^3H_6$ level within the $4f^{12}$ configuration are allowed by electric dipole selection rules, those to the higher levels, $^3P_0$, $^3P_1$, $^3P_2$, and $^1S_0$, were embedded into the strong CTS band and were too weak to be observed. As a general feature, no vibronic side bands were visible and, moreover, the number of CF transitions—even at room temperature—was very low within the different $^3H_6 \rightarrow {}^{2S+1}L_J$ transition groups.

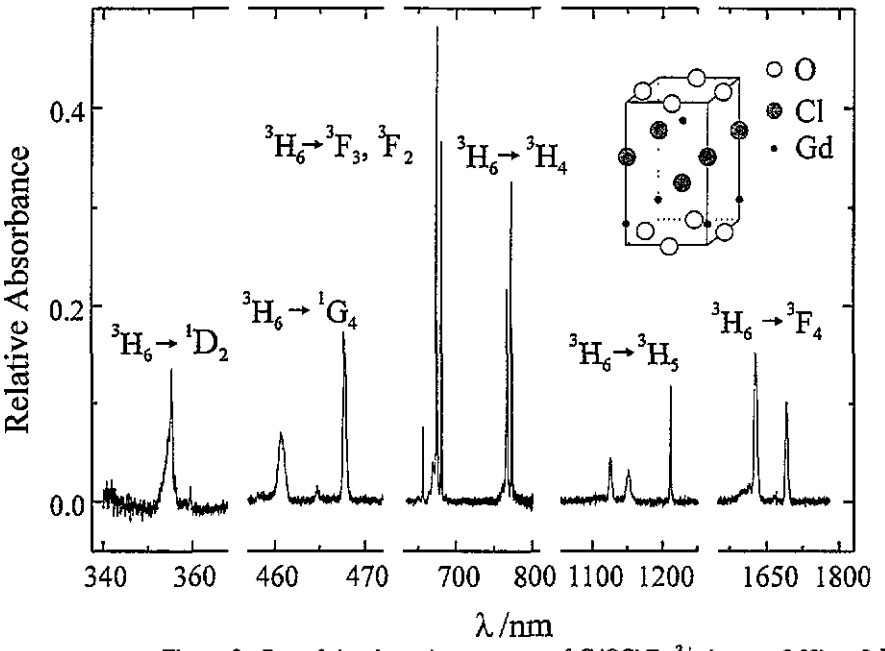

Figure 2. Part of the absorption spectrum of GdOCl:Tm^{3+} (x_{Tm} = 0.09) at 9 K. The inset depicts the contents of the tetragonal PbFCl-type unit cell of REOCl.

The analysis of the luminescence spectra had yielded three important facts: first, it was concluded that the two lowest Stark components of the $^3H_6$ ground level belong both to an irreducible representation B. The number of transitions to be observed from these levels was thus restricted to only a few in agreement with the experimental observation. Secondly, the energy difference between these two B levels is negligible and at low temperature the thermal populations of these levels are equal according to the Boltzmann distribution. This resulted in most cases in broad absorption lines which was also observed experimentally. The third level at 473 cm^{-1}, assigned to an irreducible representation E, was populated only slightly even at room temperature and hence only sparse additional information from the absorption spectrum of GdOCl:Tm^{3+} could be obtained by increasing the measuring temperature. Despite all peculiarities of the energy level scheme of Tm^{3+} in GdOCl, the absorption and luminescence spectra yielded an energy level scheme consisting of 39 levels; i.e. 55 Stark components out of the total of 91 for the whole $4f^{12}$ configuration (table 2). The sparse number of experimentally found CF levels is not unusual as a review of the literature presented above [4–23] indicated.

Table 2. Calculated and experimental energy level schemes in GdOCl:Tm^{3+}.

Level		Energy (cm^{-1}) Calc.	Exp.	Level		Energy (cm^{-1}) Calc.	Exp.
$^3H_6$	B″	0	0	$^3F_2$	E	15246	15250
	B′	1	0		A_1	15255	—
	E	453	473		B′	15396	—
	A_1	490	—		B″	15513	—
	B″	516	512				
	E	526	512	$^1G_4$	A_1	21186	21168
	A_2	557	560		A_2	21291	21338
	B′	758	—		E	21377	21381
	E	771	770		A_1	21497	21473
	A_1	785	—		B″	21522	21520
					E	21669	21704
$^3F_4$	A_1	5830	5835		B′	21844	21822
	E	5910	5912				
	B″	6004	5995	$^1D_2$	A_1	27765	27789
	A_2	6012	6005		E	27862	27813
	A_1	6073	6076		B″	28074	28080
	E	6146	6144		B′	28127	28141
	B′	6240	6239				
				$^1I_6$	B′	34259	—
$^3H_5$	E	8255	8253		B″	34259	—
	A_2	8596	—		E	34345	—
	A_1	8627	—		A_1	34621	—
	E	8678	8691		A_2	34665	—
	B′	8690	8691		E	34926	34924
	A_2	8880	—	$^3P_0$	A_1	34970	—
	E	8883	8891				
	B″	8886	8891		B′	35056	—
$^3H_4$	A_2	12700	—	$^1I_6$	B″	35413	—
	A_1	12703	—		E	35454	—
	B″	12868	12865		A_1	35484	—
	E	12966	12943				
	B′	13000	12987	$^3P_1$	E	35765	—
	E	13055	13041		A_2	36116	—
	A_1	13076	—				
				$^3P_2$	E	37808	—
$^3F_3$	A_2	14626	—		A_1	37839	—
	B′	14718	14693		B′	38100	—
	B″	14735	—		B″	38398	—
	E	14735	14735				
	E	14803	14843	$^1S_0$	A_1	74383	—

The partial energy level scheme of the Tm^{3+} ion in LaOBr [23] resembles only slightly that obtained by us. The differences may be partly due to the two different host matrices though the GdOCl and LaOBr hosts are nominally isomorphous. The non-negligibly different effect of these two hosts on the energy level scheme of the RE^{3+} ions has been previously shown for Eu^{3+} ($4f^6$ electron configuration) [26, 40]. Further discrepancies may have been caused by the difficulties encountered in [23] in distinguishing the pure electronic transitions from the vibronic side bands. The method of preparation of the samples by heating $REBr_3 \cdot xH_2O$ in air [23] must have introduced impurity phases, mainly the oxide and tribromide, which yield additional lines especially in the luminescence spectra.

3.3. Energy level simulation of the Tm^{3+} ion

The analysis of the absorption and luminescence spectra of GdOCl:Tm^{3+} provided us with 55 Stark components which set of energy level values was sufficient to enable the variation of all the free-ion (E_{0-3}, α, β, γ, and ζ_{4f}) and the five B_q^k CF parameters without imposing any restrictions. The simulation of the energy level scheme was carried out with a satisfactory RMS deviation, 21 cm^{-1}, due to the low number of experimentally observed levels. However, no large discrepancies between the calculated and experimental energy values of the individual levels could be observed which indicated the correct assignment of the levels (table 2). The quality of the fit was reflected also by the low estimated standard deviations of the parameter values reproduced in table 3. The B_0^2, B_0^4, B_4^4, and B_0^6 parameters assumed high values, whereas the B_4^6 parameter was close to zero. These values are similar to those obtained for the next-closest RE^{3+} ion (Tb^{3+}) studied so far in the GdOCl matrix [27]. The absolute signs of the B_4^4 and B_4^6 parameters could not be determined because the B_1 and B_2 levels cannot be distinguished for the C_{4v} site symmetry even carrying out measurements utilizing polarized light with single-crystal samples.

Table 3. Comparison of the free-ion and CF parameter sets (in cm^{-1}) for different REOCl or GdOCl:RE^{3+}. The values in parenthesis refer to the estimated standard deviation of the parameters.

			GdOCl:RE^{3+}		
Parameter	PrOCl [24]	NdOCl [25]	Eu^{3+} [26]	Tb^{3+} [27]	Tm^{3+}
E_0	5368(2)	11 616(36)			17 679(2)
E_1	4496(2)	4697(7)			6717(3)
E_2	21.74(2)	22.92(4)			33.69(2)
E_3	456.8(1)	471.2(15)			660.0(3)
α	23.6(1)	19.6(3)			18.37(8)
β	−676(2)	−647(12)			−887(11)
γ	[1422]	1791(29)			1935(18)
ζ_{4f}	742(1)	870(2)			2616(1)
B_0^2	−842(9)	−920(19)	−907(6)	−943(2)	−1135(15)
B_0^4	−550(24)	−333(54)	−655(10)	−634(4)	−777(29)
B_4^4	±826(16)	±819(36)	±849(8)	±649(3)	±851(19)
B_0^6	1092(37)	934(47)	976(13)	787(5)	673(37)
B_4^6	±27(27)	±209(45)	±441(9)	±264(4)	±46(26)
S^a	374	367	398	320	417
σ	17	20	4	8	21
No of Stark levels	68/91	105/182[b]	27/49	44/49	55/91

[a] The CF strength parameter S is defined as follows [44]:

$$S = \left(\frac{1}{3}\sum_k \frac{1}{2k+1}\left[(B_0^k)^2 + 2\sum_{q>0}((B_q^k)^2 + (S_q^k)^2)\right]\right)^{1/2}.$$

[b] Kramers doublets.

The CF simulation of the energy level scheme of the Tm^{3+} ion in LaOBr [23] has yielded a B_q^k parameter set completely different from that obtained in the present investigation. The discrepancy is mainly based on the different energy level scheme in [23] which, however, is based on rather unreliable spectral data. Further differences arise from the use of the incomplete basis set of 54 CF levels instead of the complete set of 91 employed by us.

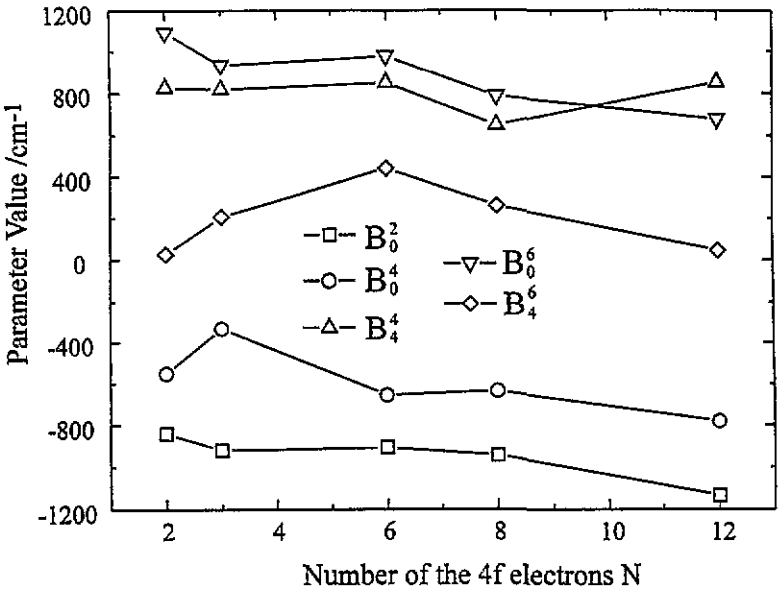

Figure 3. The evolution of the CF parameters in the REOCl or GdOCl:RE^{3+} series for YOCl:Pr^{3+} [24], NdOCl [25], GdOCl:Eu^{3+} [26], GdOCl:Tb^{3+} [27], and GdOCl:Tm^{3+} (this work).

Furthermore, in [23] the barycentres of the calculated $^{2S+1}L_J$ levels were artificially fixed to the experimental values by a set of additional parameters thus rendering the free-ion parameters physically meaningless. Some CF parameter values were deduced in [23] from the B_q^k set for YPO_4 on the grounds of structural isomorphisms between LaOBr and YPO_4 which assumption, according to structural data, has no grounds at all. Finally, the CF parameter set in [23] lacks consistency with results published earlier for other RE^{3+} ions in similar hosts. This problem has been discussed and warned of in detail by Carnall *et al* [5].

The systematics in the free-ion parameters for the RE^{3+} series in REOCl cannot be scrutinized in detail since the data are still too limited. However, a clear increase in the electrostatic interaction (the Racah parameters) and in the spin–orbit coupling can be observed toward the heavier RE^{3+} ions (table 3). The trends in the configuration interaction terms α, β, and γ are less clear and may depend on the inclusion of the Judd T^k parameters describing the three-body configuration interactions. These parameters are, however, not utilizable for the $4f^2$ and $4f^{12}$ electron configurations.

The evolution of the CF parameter values for REOCl or GdOCl:RE^{3+} as a function of the number of the 4f electrons (N) is rather smooth (figure 3) despite the host lattices being different for most of the RE^{3+} ions studied. Due to the increased nuclear charge experienced by the electrons with increasing N the B_q^k values are expected to decrease. According to simple reasoning in line with the point charge model, the magnitude of the decrease of the CF effect is given by the equation $B_q^k = A_q^k\langle r^k\rangle$ where the lattice sums A_q^k and the radial integral values $\langle r^k\rangle$ depend on the host lattice and on the RE^{3+} ion, respectively [41]. For the GdOCl lattice the A_q^k values can be considered as constant irrespective of the dopant whereas the values of the radial integrals [45] decrease considerably from Pr^{3+} to Tm^{3+}. Such a trend cannot be observed in the REOCl:RE^{3+} series (figure 3) though a few parameters decrease up to the $4f^6$ electron configuration (Eu^{3+} ion). However, the screening and expansion factors σ_k and τ, respectively, may dampen the decrease in the $\langle r^k\rangle$ factors [41].

Beyond the middle of the RE^{3+} series, other factors, e.g. the energy of the 5s (and 5p) orbitals as well as the two-electron CF terms, may have additional influence on the CF parameter values. In principle, the lowering of the 5s orbital energy should strengthen the CF effect by increasing the mixing of the opposite parity 5s terms to the 4f wave functions. Such a trend can indeed be observed for most of the parameter values beyond Eu^{3+} (figure 3). The two-electron effects including both the orbitally correlated (LCCF) [13] and the spin-correlated CF (SCCF) interactions [46] may have some importance, too, though, e.g. for Gd^{3+} and Ho^{3+} in LaF_3 [47], the influence of SCCF has been considered close to negligible.

From a theoretical point of view, the use of additional parameters taking into account some of the two-electron correlation effects may be advantageous. In practice, however, the number of parameters to be included in calculations is too large requiring thus the use of some simplifications and rejection of the less important parameters. The theoretical means of showing which parameters should be omitted is not totally clear, and the experimental verification of the choice seems at the moment not too certain due to the inherent inadequacies of the basic parametrization scheme. For the REOCl:RE^{3+} system more data are needed for both the lighter (Sm^{3+}) and the heavier RE^{3+} (Dy^{3+}, Ho^{3+}, and Er^{3+}) ions before such a verification can be carried out. Further work is in progress in order to obtain the additional data required.

4. Conclusions

The 55 CF components of the nine lowest $^{2S+1}L_J$ multiplets of the Tm^{3+} ion in the GdOCl matrix were derived from the analysis of the optical absorption and luminescence spectra measured at selected temperatures down to 9 K. The energy level scheme was simulated with a Hamiltonian including the parametrized electrostatic (the Racah parameters E_{0-3}) and the two-body configuration interactions (the Trees parameters α, β, and γ) as well as the spin–orbit coupling (the coupling constant ζ_{4f}) in addition to the effect of the neighbouring ions according to a crystal field of C_{4v} symmetry. All 13 parameters including the five B_q^k parameters (B_0^2, B_0^4, B_4^4, B_0^6, and B_4^6) were refined without restrictions imposed on any parameter and their values were determined unambiguously (except for the absolute signs of B_4^4 and B_4^6) simultaneously by least-squares calculations. The RMS deviation of 21 cm^{-1} achieved in the simulation is good taking into account the restricted degrees of freedom due to the limited basis set of experimentally observed levels. The B_q^k set describes well the energy level scheme of GdOCl:Tm^{3+} and was, moreover, found to be consistent with those obtained for the Pr^{3+}, Nd^{3+}, Eu^{3+}, and Tb^{3+} ions in the REOCl or REOCl:RE^{3+} series.

In addition to deriving information on the importance of the different free-ion and CF interactions on the energy level scheme of the Tm^{3+} ion in REOCl matrices, the parameter set obtained can be employed as predicting the effect of the said interactions on the other RE^{3+} ions. This may overcome the difficulties in deriving information from too severely restricted data and avoid any physically meaningless parametrization.

Acknowledgments

Financial support by the Academy of Finland (project No 4966) of JH and by the Ministry of Education and University of Turku of R-JL is gratefully acknowledged.

References

[1] Blasse G 1993 *J. Alloys Compounds* **192** 17
[2] Caird J A, DeShazer L G and Nella J 1975 *IEEE J. Quantum Electron.* **QE-11** 874
[3] Lenth W and Macfarlane R M 1992 *Opt. Photon News* **3** 8
[4] Morrison C A and Leavitt R P 1979 *J. Chem. Phys.* **71** 2366
[5] Carnall W T, Goodman G L, Rajnak K and Rana R S 1989 *J. Chem. Phys.* **90** 3443
[6] Jensen H P, Linz A, Leavitt R P and Morrison C A 1975 *Phys. Rev.* B **11** 92
[7] Esterowitz L, Bartoli F J, Allen R E, Wortman D E, Morrison C A and Leavitt R P 1979 *Phys. Rev.* B **19** 6442
[8] Muto K 1973 *J. Chem. Phys. Solids* **34** 2029
[9] Gruber J B, Leavitt R P and Morrison C A 1981 *J. Chem. Phys.* **74** 2705
[10] Jayasankar C K, Richardson F S and Reid M F 1989 *J. Less-Common Metals* **148** 289
[11] Dieke G H 1968 *Spectra and Energy Levels of Rare Earth Ions in Crystals* (New York: Interscience) p 310
[12] Stöhr J, Olsen D N and Gruber J B 1971 *J. Chem. Phys.* **55** 4463
[13] Yeung Y Y and Newman D J 1987 *J. Chem. Phys.* **86** 6717
[14] Gruber J B, Leavitt R P, Morrison C A and Chang N C 1985 *J. Chem. Phys.* **82** 5373
[15] Karayianis N, Wortman D F and Morrison C A 1976 *Solid State Commun.* **18** 1299
[16] Morrison C A, Karayianis N and Wortman D F 1977 *Harry Diamond Laboratories Report* HDL-TR-1788
[17] Gruber J B, Hills M E, Macfarlane R M, Morrison C A, Turner G A, Quarles G J, Kintz G J and Esterowitz L 1989 *Phys. Rev.* B **40** 9464
[18] Wortman D F, Leavitt R P and Morrison C A 1974 *J. Chem. Phys. Solids* **35** 591
[19] Karayianis N, Morrison C A and Wortman D F 1976 *Harry Diamond Laboratories Report* HDL-TR-1776
[20] Wortman D F, Morrison C A and Leavitt R P 1975 *Phys. Rev.* B **12** 4780
[21] Kato Y and Takada H 1979 *Bull. Chem. Soc. Japan* **52** 990
[22] Porcher P and Charreire Y 1983 *J. Electrochem. Soc.* **130** 175
[23] Mazurak Z, Garcia A and Fouassier C 1994 *J. Phys.: Condens. Matter* **6** 2031
[24] Antic-Fidancev E, Hölsä J, Lemaitre-Blaise M and Porcher P 1991 *J. Chem. Soc.: Faraday Trans.* **87** 3625
[25] Beaury L 1988 *PhD Thesis* Université de Paris-Sud, Orsay, France p 128
[26] Hölsä J and Porcher P 1981 *J. Chem. Phys.* **75** 2108
[27] Hölsä J and Porcher P 1982 *J. Chem. Phys.* **76** 2798
[28] Hölsä J and Niinistö L 1980 *Thermochim. Acta* **37** 155
[29] Templeton D H and Dauben C H 1953 *J. Am. Chem. Soc.* **75** 6069
[30] Castellanos M and West A R 1980 *J. Chem. Soc.: Faraday Trans.* **76** 2159
[31] Henry N F M and Lonsdale K (ed) 1969 *International Tables for X-ray Crystallography* vol 1 (Birmingham: Kynoch)
[32] Sillén L G and Nylander A-L 1941 *Svensk Kem. Tidskr.* **53** 367
[33] Caro P 1968 *J. Less-Common Metals* **16** 367
[34] Beck H P 1976 *Z. Naturf.* **316** 1562
[35] Wilmarth W R and Peterson J R 1991 *Handbook of Physics and Chemistry of Actinides* ed A J Freeman and C Keller (Amsterdam: Elsevier) p 1
[36] Wybourne B G 1965 *Spectroscopic Properties of Rare Earths* (New York: Interscience)
[37] Porcher P 1988 *Phase Transitions* **13** 233
[38] Prather J L 1961 *NBS Monograph* 19
[39] Porcher P 1989 unpublished
[40] Hölsä J and Porcher P 1982 *J. Chem. Phys.* **76** 2790
[41] Hölsä J and Kestilä E 1995 *J. Alloys Compounds* at press
[42] Hase Y, Dunstan L and Temperini M L A 1981 *Spectrochim. Acta* A **37** 597
[43] Blasse G, de Mello Donega C and Meijerink A 1994 *2nd Int. Conf. on f-Elements (ICFE-2) (Helsinki)* (Jyvaskylä: Gummerus) p 199
[44] Chang N C, Gruber J B, Leavitt R P and Morrison C A 1982 *J. Chem. Phys.* **76** 3877
[45] Freeman A J and Desclaux J P 1979 *J. Magn. Magn. Mater.* **12** 11
[46] Reid M F and Richardson F S 1985 *J. Chem. Phys.* **83** 3831
[47] Reid M F 1987 *J. Chem. Phys.* **87** 2875